Article

Cell Reports

Extremely Long-Range Chromatin Loops Link Topological Domains to Facilitate a Diverse Antibody Repertoire

Graphical Abstract

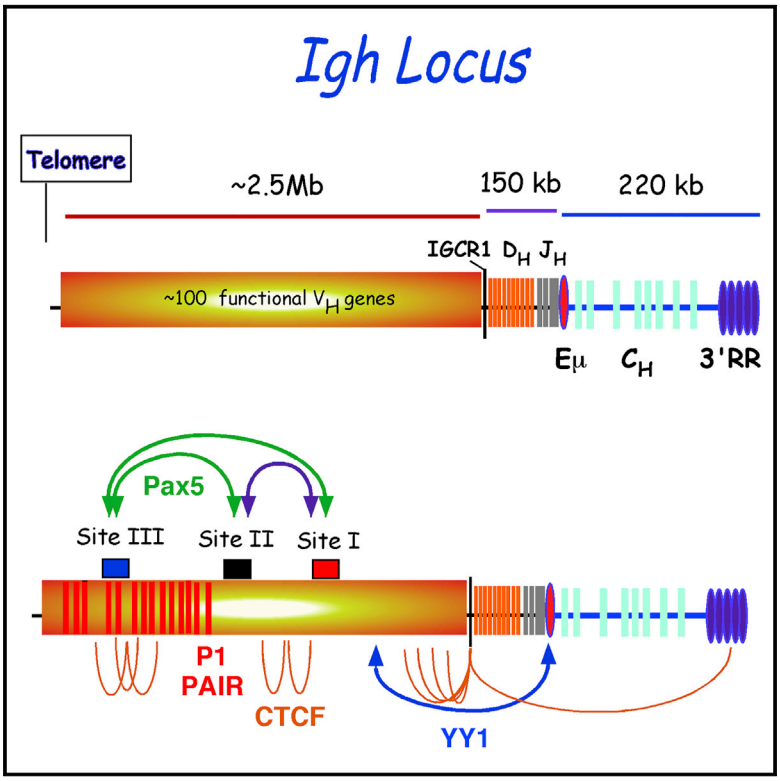

Authors

Lindsey Montefiori, Robert Wuerffel, Damian Roqueiro, ..., Jie Liang, Ranjan Sen, Amy L. Kenter

Correspondence

senranja@grc.nia.nih.gov (R.S.), star1@uic.edu (A.L.K.)

In Brief

Using chromosome conformation capture technology, Montefiori et al. define the molecular architecture supporting large-scale Igh locus contraction at the pro-B cell stage of development. Pax5 deficiency leads to loss of a subset of these long chromatin loops suggesting a multilayered mechanism by which V_H gene usage is controlled.

Highlights

- Igh locus contraction occurs in pro-B cells prior to VDJ joining
- Pro-B cell-specific chromatin looping at the multi-megabase scale defines locus contraction
- A subset of these exceptionally long chromatin loops are Pax5 dependent
- VH gene rearrangement is dependent upon independently regulated chromatin topologies

Accession Numbers

GSE76086

Montefiori et al., 2016, Cell Reports *14*, 896–906
February 2, 2016
http://dx.doi.org/10.1016/j.celrep.2015.12.083

OPEN ACCESS
CellPress

Cell Reports
Article

Extremely Long-Range Chromatin Loops Link Topological Domains to Facilitate a Diverse Antibody Repertoire

Lindsey Montefiori,[1,6] Robert Wuerffel,[2,6] Damian Roqueiro,[3] Bryan Lajoie,[4] Changying Guo,[1] Tatiana Gerasimova,[1] Supriyo De,[5] William Wood,[5] Kevin G. Becker,[5] Job Dekker,[4] Jie Liang,[3] Ranjan Sen,[1,7,*] and Amy L. Kenter[2,7,*]

[1]Gene Regulation Section, Laboratory of Molecular Biology and Immunology, National Institute on Aging/National Institutes of Health, Baltimore, MD 21224, USA

[2]Department of Microbiology and Immunology, University of Illinois College of Medicine, Chicago, IL 60612-7344, USA

[3]Department of Bioengineering, University of Illinois College of Engineering and College of Medicine, Chicago, IL 60612-7344, USA

[4]Howard Hughes Medical Institute and Program in Systems Biology, Department of Biochemistry and Molecular Pharmacology, University of Massachusetts Medical School, Worcester, MA 01605-0103, USA

[5]Gene Expression and Genomics Unit, Laboratory of Genetics, National Institute on Aging/National Institutes of Health, Baltimore, MD 21224, USA

[6]Co-first author

[7]Co-senior author

*Correspondence: senranja@grc.nia.nih.gov (R.S.), star1@uic.edu (A.L.K.)

http://dx.doi.org/10.1016/j.celrep.2015.12.083

SUMMARY

Early B cell development is characterized by large-scale *Igh* locus contraction prior to V(D)J recombination to facilitate a highly diverse Ig repertoire. However, an understanding of the molecular architecture that mediates locus contraction remains unclear. We have combined high-resolution chromosome conformation capture (3C) techniques with 3D DNA FISH to identify three conserved topological subdomains. Each of these topological folds encompasses a major V_H gene family that become juxtaposed in pro-B cells via megabase-scale chromatin looping. The transcription factor Pax5 organizes the subdomain that spans the V_HJ558 gene family. In its absence, the J558 V_H genes fail to associate with the proximal V_H genes, thereby providing a plausible explanation for reduced V_HJ558 gene rearrangements in Pax5-deficient pro-B cells. We propose that *Igh* locus contraction is the cumulative effect of several independently controlled chromatin subdomains that provide the structural infrastructure to coordinate optimal antigen receptor assembly.

INTRODUCTION

The mechanisms that govern V gene usage in VDJ rearrangements are central to understanding the formation of the BCR and TCR repertoires. Chromatin conformation and coordinated chromosomal movements govern the clustering of genes in transcription machines and the matrix of interactions specifying regulatory element associations. The *Igh* locus undergoes several different chromosomal movements that ensure developmental-stage and lineage-specific DNA recombination and transcription including relocation from the nuclear periphery to the center and re-organization of the *Igh* locus chromatin topology during B cell ontogeny (Fuxa et al., 2004; Kosak et al., 2002; Sayegh et al., 2005). In the mouse, there are ~100 functional V_H gene segments that are scattered over 2.5 Mb of the *Igh* locus that must recombine with a rearranged DJ_H element assembled from 1 of 8–12 D_H and one of four J_H gene segments. In primary pro-B cells of the bone marrow (BM), RAG recombinase mediates V(D)J or VJ joining for both Ig H and L chain genes. However, the molecular mechanism by which the distal V_H genes gain spatial proximity to the rearranged D_HJ_H gene segments remains obscure.

Chromatin compaction has been studied extensively by cytological methods. Three-dimensional (3D) DNA fluorescent in situ hybridization (FISH) studies in pro-B cells indicate that the Igh locus contracts, and this process is inferred to juxtapose distal V_H genes near to proximal D_H segments to promote V(D)J joining (Fuxa et al., 2004; Jhunjhunwala et al., 2008; Kosak et al., 2002). Locus contraction requires the transcriptional regulators, Pax5, YY1, and Ikaros (Fuxa et al., 2004; Liu et al., 2007; Reynaud et al., 2008). Loss of Igh locus compaction is correlated with the biased usage of the proximal V_H gene segments (Hesslein et al., 2003). The degrees of locus compaction are inferred from relationships of interprobe nuclear distances versus genomic distances. However, FISH-based measurements have limited resolution (100–1,000 nm), and it has been difficult to ascertain the identity of specific DNA sequences that mediate locus contraction. The advent of chromosome conformation capture (3C) and related methods allows examination of pairwise chromatin interactions at the molecular level (~1–100 nm) in cell populations (Gibcus and Dekker, 2013). 3C-based methods can delineate long-range chromatin looping interactions and have

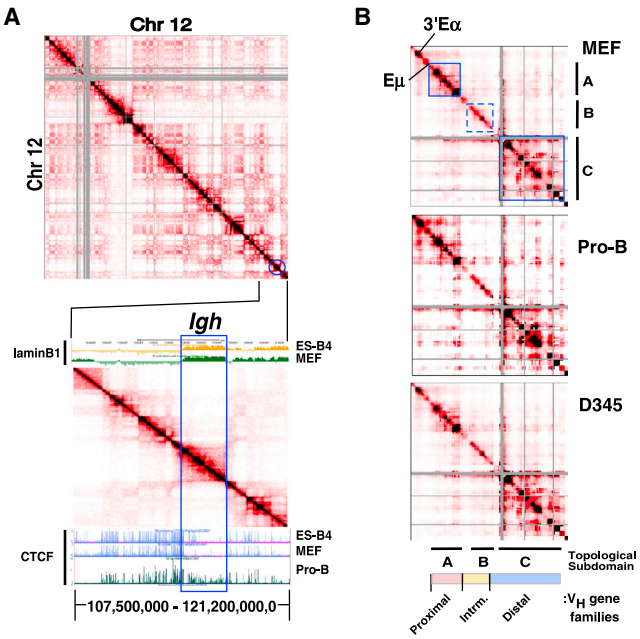

Figure 1. The *Igh* Locus Partitions into a 2.9-Mb TAD and Conserved Topological Subdomains

(A) (Upper panel) Normalized HiC interaction frequencies from an AMuLV pro-B cell line (adapted from Zhang et al., 2012) representing chromosome 12 is displayed as a 2D heatmap binned at 100 kb resolution. HiC sequencing reads are indicated by the color (red) intensity from interacting pairs of Hind III fragments. Gray pixels indicate areas of low uniquely mapped reads or regions with many large restriction fragments (>100 kb). (Lower panel) HiC data from chromosome 12 (107,500,000–121,200,000,0; mm9) are shown aligned to a UCSC Genome Browser snapshot showing chromatin immunoprecipitation sequencing (ChIP-seq) for CTCF (Lin et al., 2012) and Dam-ID lamin B1 data (Peric-Hupkes et al., 2010) in the indicated cell types.

(B) 5C analyses of the 2.9-Mb *Igh* locus in MEF, Rag-deficient pro-B cells, and the AMuLV pro-B cell line, D345. Normalized 5C data underwent binning analysis (bin size, 150,000 kb; step size, 15 kb). Topological subdomains A and C are indicated by the solid blue outline and B by dashed blue lines. The heatmaps are scaled as follows: MEF 37-1840, Rag2$^{-/-}$ pro B cells: 19-1254, D345: 89-6355.

been successfully used to reveal large-scale chromatin organizations that are congruent with FISH studies (Bickmore and van Steensel, 2013). However, looping interactions specifying locus contraction remain poorly defined, and one recent study has suggested that distal V_H gene contacts with D_HJ_H elements are stochastic (Medvedovic et al., 2013).

Chromosomes are organized into higher-order spatial architectures of multiple length scales (Gibcus and Dekker, 2013). Independent compartments of euchromatin and heterochromatin form at intermediate length scales of 1–10 Mb within chromosomal territories (Lieberman-Aiden et al., 2009). Chromatin is further organized into megabase-sized topologically associating domains (TADs) that represent spatial zones of high-frequency self-interacting chromatin contacts (Dixon et al., 2012; Nora et al., 2012). Many TADs show a high degree of alignment with discrete transcriptionally repressive nuclear lamina-associated domains (LADs) that occur at variable stages of development (Nora et al., 2012). Although TADs are conserved between mouse and human and are invariant during development, focal facultative chromatin folding regulating gene expression can occur on the sub-megabase scale without changing TAD organization (Dixon et al., 2012; Nora et al., 2012). We reasoned that mapping *Igh* locus chromatin topologies might allow identification of functional long-range interactions and their underlying loop anchors that mediate locus contraction.

Here, we examine the relationship between higher-order chromatin structure and gene function at several levels using the 3C-based methodology, chromosome conformation capture carbon-copy (5C), in combination with 3D DNA FISH. We find that the *Igh* locus spans a multi-megabase-sized topological fold that, in turn, corresponds remarkably well to the previously described *Igh* LAD (Zullo et al., 2012). We find a nested hierarchy of constitutive chromatin interactions that serve to structure conserved sub-topologies within the *Igh* topological fold that range in size from ~0.44 to 1.1 Mb. At the pro-B cell stage of development, these subdomains achieve spatial proximity by means of chromatin looping over multi-megabase-scale distances to collectively generate locus contraction. We find that the transcription factor Pax5 is required for specific pro-B cell looping interactions, and these contacts are independent of the *cis*-regulatory element, Eμ. We provide a molecular definition of locus contraction by identifying loop anchor sites that are key mediators of this process and consider the functional implications of hierarchical layers of chromatin folding and compaction on V_H gene usage and IgH diversity.

RESULTS

The *Igh* Locus Is Organized as a Compartment with Several Sub-topological Domains

Comprehensive genome-wide mapping of chromatin architecture using HiC is based on proximity ligation chromosome conformation capture (3C) assays and permits visualization of higher-order chromosomal landscapes (Lieberman-Aiden et al., 2009). To gain insight into the chromatin organization of the *Igh* locus, HiC data for chromosome 12 from an AMuLV pro-B cell line (Zhang et al., 2012) and embryonic stem (ES) cells (Dixon et al., 2012) generated in a different studies were analyzed. The 2D interaction matrices constructed using 100-kb binning analyses shows all pairwise interaction frequencies captured by HiC along chromosome 12 for the pro-B cell line (Figure 1A, upper panel). The diagonal reflects interaction frequencies along the chromosome between fragments that are neighbors in the genome, whereas color off the diagonal represents long-range looping interactions. The frequency of interactions is inversely related to the genomic distance separating the pair of restriction fragments. The *Igh* locus, indicated by the blue circle, is located close to the telomeric end of chromosome 12 (Figure 1A, upper panel). TADs are discrete blocks, spanning on average 0.8 Mb in mammalian cells and range up to several megabases, within which the pairwise contacts are relatively frequent and are relatively conserved between cell types (Dixon et al., 2012; Nora et al., 2012). TADs are visible along the diagonal of chromosome 12 and are readily evident in an expanded view of the HiC heatmap (Figure 1A, lower panel). Compartments are large chromosomal domains spanning

several megabases that preferentially interact with other compartments (Lieberman-Aiden et al., 2009) and are visible as a plaid pattern off the diagonal (Figure 1A, upper panel). Compartments tend to be cell type or differentiation stage specific. The *Igh* locus is encompassed within a single 2.9-Mb self-associating domain that is pro-B cell stage specific as it is absent in ES cells (Figure 1A, lower panel; also see Figure S1). However, the *Igh* domain is also a relatively autonomous unit since it interacts infrequently with other compartments (Figure 1A, upper panel). Thus, *Igh* topological fold is largely insulated from other chromosome 12 contacts. We refer to the spatial arrangement of the Igh locus as an insulated topological fold (i-TOF).

The *Igh* locus is associated with the nuclear lamina (NL) in non-lymphoid cells and multipotent progenitors but relocates away from the NL to the transcriptionally permissive nuclear center in lineage committed pro-B cells (Zullo et al., 2012). We investigated the relationship between the *Igh* i-TOF and LAD by leveraging previously constructed maps of genome-NL interactions established using laminB1 (LMNB1) DNA adenine methyltransferase identification (DamID) protocols (Peric-Hupkes et al., 2010; Zullo et al., 2012). We aligned LMNB1-DamID maps along with HiC data from a segment of chromosome 12 that spans the *Igh* locus and its flanking regions (Figure 1A, lower panel). In embryonic stem cells (ESC) and mouse embryonic fibroblasts (MEF), the *Igh* LAD is essentially coincident with the *Igh* locus as indicated by the blue rectangle (Figure 1A, lower panel; also see Figure S2 and Table S1). Furthermore, in MEF and ESC, the activating histone modifications H3K4me1 and H3K27Ac are underrepresented throughout the transcriptionally silent *Igh* LAD, whereas these marks are present in flanking regions (Figure S2). In marked contrast, H3K4me1 is enriched across the transcriptionally active *Igh* locus in pro-B cells (Figure S2), and the LAD is absent (Zullo et al., 2012). Our finding that the *Igh* LAD and i-TOF are coincident is intriguing since it implies that developmentally regulated DNA elements differentially contribute to chromatin organizational features supporting LAD and i-TOF scaffolds.

A counterpoint to the loss of *Igh* LAD NL-association in pro-B cells is the acquisition of CTCF and cohesin (Rad21) binding. CTCF is an architectural protein that contributes to the establishment of a 3D spatial organization of chromatin fibers and to *Igh* locus compaction (Degner et al., 2011; Guo et al., 2011a). Cohesin is a highly conserved multiprotein complex that includes Rad21, functions during DNA replication to mediate the association of sister chromatids, and is an interaction partner with CTCF (Seitan and Merkenschlager, 2011). Using publically available datasets, we observe that CTCF decorates the *Igh* locus in pro-B cells, and its binding largely coincides with the cohesin subunit, Rad21, in accord with earlier studies (Figure 1A, lower panel; also see Figure S2) (Degner et al., 2009). CTCF occupancy is greatly diminished in MEF, as previously noted (Degner et al., 2009), as well as in ESC, and thymus (Figure 1, lower panel; Figure S1). The absence of CTCF binding was not due to a technical failure of the assay since CTCF abundance was high in region flanking the *Igh* locus for ESC, MEF, and thymus (Figure 1A, lower panel; Figure S1). Genome-wide CTCF binding occurs both at invariant sites that are conserved between species and tissues and at sites that show cell-type-specific distribution (Cuddapah et al., 2009). It is striking therefore that occupancy of the *Igh* locus with CTCF, Rad21, and activating histone marks occurs across the entire i-TOF and is contemporaneous with disengagement from the NL. These observations strongly imply that the *Igh* LAD provides a regulated framework in which alterations in nuclear positioning and chromatin structure occur in a domain-wide fashion during B cell development.

Unique Topological Substructures in the *Igh* Locus

To examine cell-type-specific patterns of higher-order chromatin organization in the *Igh* locus at high resolution, we performed 5C in a massively parallel manner at distinct stages of B cell development. 5C, a high-throughput derivative of 3C, involves selective amplification of chromatin interactions captured by proximity ligation and permits definition of chromatin structure at the level of single restriction fragments (Figure S3A). An alternating forward and reverse 5C primer design interrogated in *cis* over 12,000 potential *Igh* long-range interactions and 525 interactions at the chromosome 5 gene desert, using two biological replicates of MEFs and Rag-deficient pro-B cells, as described (Kumar et al., 2013) and an Abelson-transformed Rag2-deficient pro-B cell line, D345 (Figure S3B). We assessed our 5C results by examining the consistency between biological replicates. Heatmaps of our raw 5C data were similar for biological replicates at both the *Igh* locus and the chromosome 5 gene desert (Figure S3C). 5C signals were well correlated between biological replicates (pro-B 1 versus pro-B 2, Spearman correlation coefficient 0.723; MEF1 versus MEF2, Spearman correlation coefficient 0.888) when considering counts for all fragment combinations and indicate that the 5C libraries are high quality and consistent between replicates.

We visualized the normalized 5C heatmaps for MEF, Rag2-deficient pro-B cells, and the D345 cell line (Figure 1B; also see Table S2). The 5C data were submitted to binning analyses over 150 kb revealing that high-density chromatin contacts occurred preferentially within two subdomains A and C, ~0.44 and 1.2 Mb, respectively, indicated by the intense red color and demarcated by the blue boxes (Figure 1B). A weaker set of interactions occurred within subdomain B (indicated by the dashed blue box). The overall locations and sizes of the subdomains are conserved in MEFs, pro-B cells, and D345 cells indicating constancy of genomic folding patterns in different cell types (Figure 1B). However, in primary pro-B cells subdomain A also appears to encompass the 3′ end of the *Igh* locus including the B-cell-specific 3′Eα enhancer and highlights potential lineage-specific looping interactions (Figure 1B). The disposition of the 3′Eα enhancer is examined in greater detail in the sections below where direct sample to sample comparison of 5C interaction frequencies are analyzed.

We next examined the distribution of V_H gene families with respect to *Igh* topological folds. The C57Bl/6 mouse strain contains 195 V_H genes that are arrayed across ~2.4 Mb of the *Igh* locus (Johnston et al., 2006). The J558 gene cluster, located at the distal 5′ end of the locus, is the largest grouping of V_H exons (Figure 1B). The 7183 V_H gene family comprises the next largest group (~0.4 Mb) and is situated at the proximal end of the locus closely abutting the D_H segment cluster. The intermediate V_H genes are composed of ten smaller families of V_H genes

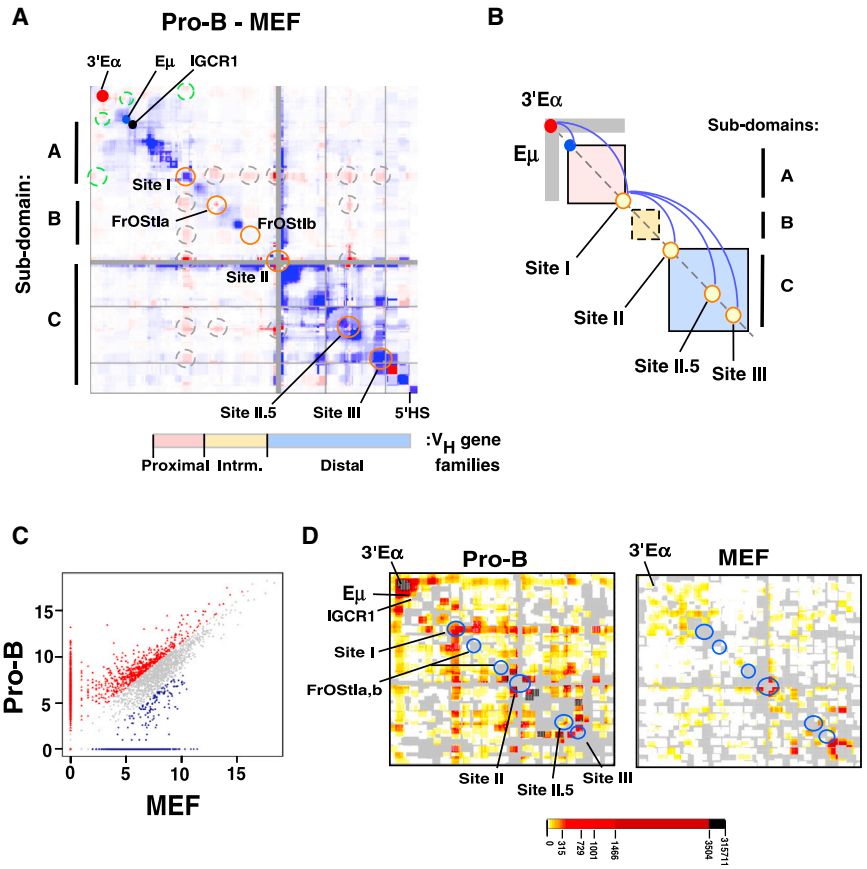

Figure 2. Developmentally Programmed Reorganization of the *Igh* Locus Chromatin Architecture in Pro-B Cells

(A) A difference plot (pro-B cells minus MEF) was calculated using normalized 5C signals (150-kb bins, 15-kb step). Elevated 5C reads in pro-B (red intensities) or MEF (blue intensities) or constitutive (white). Dots are 3′Eα (red), Eμ (blue), and IGCR1 (black). Looping interactions associated with 3′Eα (dashed green circles). Sites I (115,100,000–115,239,000; 139 kb), II (115,949,000–116,069,000; 120 kb), II.5 (116,665,000–116,770,000; 105 kb), III (116,784,000–116,874,000; 90 kb), FrOStIa (115,411,000–115,451,000; 40 kb), and FrOStIb (115,819,000–115,859,000; 40 kb) are indicated along the diagonal (orange circles), and looping interactions off the diagonal are shown (dashed gray circles). Genomic coordinates are chr12, mm9. V_H gene families and topological subdomains A–C are indicated.

(B) A diagram of topological subdomains A (pink), B (yellow), and C (blue) boxes with Eμ and 3′Eα, as indicated. Sites I-III are shown (yellow circles). Gray rectangular arms extending from 3′Eα indicate increased interactions in pro-B cells. The pro-B-cell-specific loops are shown (blue arches).

(C) Scatterplot of 5C interactions (colored dots) (constitutive, gray; pro-B cell, red; MEF, blue). Cell-type-specific interactions were >3-fold above the constitutive frequency (see Supplemental Experimental Procedures).

(D) The pro-B and MEF-specific 5C interactions defined in (C) are plotted as 2D heatmaps (100-kb bins, 10-kb step). The frequency of 5C reads is indicated by the color key, and gray indicates the absence of interactions.

(~0.5 Mb) located between the 7183 and J558 families (Figure 1B). Topological subdomain A spans from around the intronic Eμ through the J_H and D_H clusters and includes proximal 7183 V_H genes (Figure 1B). Notably, in pro-B cells, subdomain A extends from 3′Eα enhancer and through the proximal 7183 V_H genes (Figure 1B). The 3′ end of topological subdomain C is close to the boundary for the J558 genes (Johnston et al., 2006). The two highly structured topological blocks, A and C, are separated by the less structured B interval spanning most of the intermediate V_H genes (Figure 1B). Thus, V_H gene families are discretely segregated within specific topological folds. Conservation of the topological fold structure of the *Igh* locus in MEF and pro-B cells suggests that many chromatin interactions are constitutive and conserved through mouse development. Looping interactions unique to pro-B cells could be obscured by a plethora of constitutive interactions common to MEF and primary pro-B cells.

Igh Locus Spatial Organization Defined by Constitutive and Cell-type-Specific Chromatin Contacts

We explored whether focal facultative chromatin contacts between subdomains A (D_H/J_H) and C (distal V_H) contribute to unique chromatin folding in pro-B cells. First, we constructed a difference heatmap generated by subtracting MEF from primary pro-B 5C normalized datasets to identify pro-B cell- (red intensities) and MEF- (blue intensities) specific interactions (Figure 2A). The difference heatmap allows visualization of the relative frequencies of looping interactions within pro-B and MEF chromatin samples. The heatmap is aligned with the V_H gene families and the *Igh* topological subdomains A–C, oriented along the x and y axis, respectively. We found two groups of very long-range pro-B cell-specific interactions that are indicated by the dashed circles off the diagonal (Figure 2A). The first group (green dashed circles) is anchored by 3′Eα and associates with several sites including Eμ and site I located at the 3′- and 5′ ends of topological subdomain A, respectively (Figure 2A). The second group of contacts, anchored at site I (gray dashed circles), are termed meta-long-range loops (or meta-loops) as they span exceptionally long distances between topological subdomains (Figure 2A). Looping contacts anchored at sites I, II, II.5, III, Friend of site I a (FrOStI a), and FrOStI b are enriched in the primary pro-B cells (orange circles along the diagonal) are not evident in MEF and are distinct from interactions previously noted (Guo et al., 2011a; Jhunjhunwala et al., 2008) (Figure 2A). Site I anchors chromatin looping with sites in subdomain B (FrOStI a and FrOStI b) and subdomain C (sites II, II.5, and III) containing the intermediate and distal V_H genes, respectively (Figures 2A and 2B). The simultaneous engagement of these loop anchors that span the entire *Igh* locus may be responsible for locus contraction. Sites I, II, III, and FrOStIa

display CTCF, Rad21, and Mediator1 binding. Detailed analyses of these sites are under way and will be reported separately.

To further examine the involvement of sites I-II-III in defining pro-B cell chromatin topologies, we normalized the 5C datasets using the chromosome 5 gene desert interactions as a denominator (Supplemental Information; Tables S3, S4, and S5; Figure S4). Chromatin interactions within the gene desert do not change in different cell types. Our method produces an interaction frequency that is directly comparable between experiments and permits detection of significant fragment-to-fragment looping contacts above the expected background interactions. *Igh* interactions are identified that are common to both MEF and pro-B cells (gray dots) or preferentially expressed in pro-B cells (red dots) or MEF cells (blue dots) (Figure 2C). Constitutive 5C interactions (66%; gray dots) differed less than 3-fold between MEF and pro-B cells, whereas interactions that displayed a greater than a 3-fold difference were defined as cell type specific. Interactions that were exclusively detected in pro-B or MEF cells are located along the x or y axis, respectively (Figure 2C). We examined the pro-B and MEF-specific interactions in 2D heatmaps to discover cell-type-specific looping interactions. We found that interactions involving 3′Eα were elevated in pro-B cells and were nearly undetectable in MEF (Figure 2D). Frequent chromatin contacts are detected in pro-B cells between 3′Eα with Eμ, IGCR1, and site I, and site I with FrOStIa, FrOStIb, site II.5, and site III (Figure 2D). We and others have previously noted pro-B-cell-specific chromatin looping anchored at 3′Eα and associated with Eμ and IGCR1 (Degner et al., 2009; Guo et al., 2011a, 2011b; Kumar et al., 2013). Our findings indicate that locus contraction results from pro-B-cell-specific focal facultative chromatin associations through site I and not from random compaction of the locus (Figure 2B).

Spatial Proximity of Loop-Attachment Sites I-III Is Pro-B Cell Specific

Assays based on 3C detect the average chromatin interaction frequency in a cell population. We used 3D DNA FISH to independently assess the chromatin interaction frequency between specific anchor sites in single cells. We first tested the prediction that two loci within a TAD are spatially closer to each other than two loci that are separated by the same genomic distance but situated in adjacent domains. For this, we used bacterial artificial chromosome (BAC) probes H14, RI, and RII that are separated by 877 kb (H14-RI) and 895 kb (RI-RII), respectively (Figure 3A) in quantitative 3D-FISH analyses. H14 maps 100 kb outside the 2.9-Mb *Igh* TAD indicated by Hi-C, and RI and RII correspond closely to sites I and II identified by 5C (Figure 3A). Quantitative three-color 3D-FISH analyses in primary pro-B cells from RAG2-deficient mice showed that spatial distances between RI-RII probes were, on average, significantly smaller than H14-RI inter-probe distances (Figures 3B–3D). These observations confirmed that sites I and II lay within the *Igh* i-TOF, whereas H14 did not. The frequent superposition of probes RI and RII in pro-B cells (approximately 70% of nuclei examined) strongly supported the identification of long-distance interactions between sites I and II by 5C.

5C analysis indicated that long distance interactions between sites I, II, and III were enriched in pro-B cells and underrepresented in MEFs (Figure 2). To independently assess cell lineage specificity of these interactions, we performed 3D-FISH using Rag2-deficient pro-B and non-B lineage cells. BAC probe RIII corresponded closely to site III identified by 5C, and the three probes were separated by equidistant genomic intervals (Figure 3A). All three pairwise FISH signals between probes RI-RII, RII-RIII, and RI-RIII were essentially super-imposed in 60%–80% of pro-B cell alleles (Figures 3E–3H; also see Table S6). This was most remarkable for RI-RIII interactions where the probes are located almost 2 Mb apart. In contrast, probes RI-RIII were spatially clustered in only approximately 18% of non-B lineage cells (Figures 3E and 3F), suggesting a major reduction in co-location. However, there is also a degree of intrinsic association that was independent of cell lineage. The conserved topological subdomains that are supported by constitutive chromatin interactions in MEFs and pro-B cells may be the basis for underrepresentation, but not absence, of these interactions.

To further examine the proposition that sites I-II-III represented preferred pro-B-specific interaction sites, we used a probe, R.I.5, that lies between RI and RII in FISH assays (Figure S5A). If looping is random, then genomic proximity of probes RI.5-RII (separated by 451 kb) would favor their pairwise association compared to RI-RII (separated by 895 kb) or RII-RII.5 (separated by 685 kb). Site II.5, co-located with FISH probe RII.5, is situated in subdomain C and is predicted to interact with site II based on our 5C analyses (Figure 3). We found that RI-RII and RII-RII.5 probe interactions were similar in pro-B cell alleles. Notably, the spatial separation between R1.5-RII was significantly greater than either of the other two interactions (Figures S5B and S5C), further strengthening the notion that sites I, II, and III represented preferred, rather than random interaction sites.

Spatial Organization of the *Igh* Locus Is Configured by Three-Way Looping of Sites I-II-III

Because 5C assays assess chromatin interactions in populations of cells, our 5C studies did not distinguish between pairwise or more complex interactions among multiple interacting sites. However, the high frequency of pairwise interactions between sites I-II, II-III, and I-III strongly suggested that these sites interact with each other simultaneously (Figure 3). To directly assess the frequency of three-way long-distance interactions, we performed three-color 3D-FISH with RI (red), RII (green), and RIII (blue) in primary pro-B cells (Figure 4A). Guidelines used to score allele configurations in three-color FISH assays are described (Figure S6). Our FISH studies indicated that loop anchor sites I, II, and III were superimposed in three-way interactions in a high proportion (31.5%) of pro-B cell alleles and were spatially close on an additional 29% of alleles (Figure 4B, insets a and a.1). Superimposed probes are indicative of molecular contacts (Belmont, 2014). Conversely, probes RI-RII-RIII were spatially separated on only 1% of alleles in pro-B cells (Figure 4B, inset e). We infer that sites I–III engage in three-way interactions in a high proportion of pro-B cells.

The pattern of probe interactions found in pro-B cells was reversed in primary non-B lineage cells from the bone marrow. Here, probes RI-RII-RIII overlapped on only 5.0% of alleles, relative to 31% in pro-B cells, and were spatially close on an

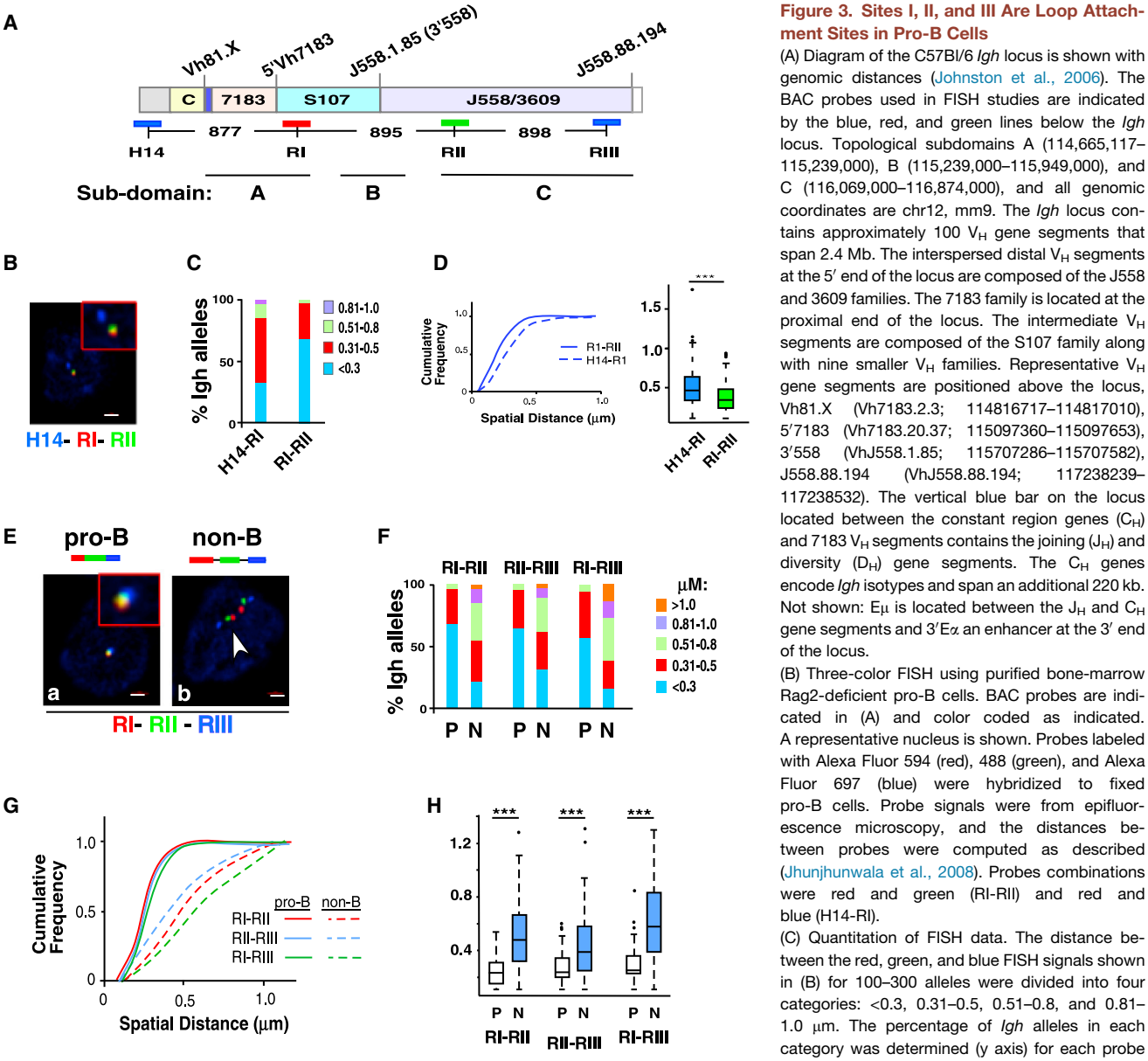

Figure 3. Sites I, II, and III Are Loop Attachment Sites in Pro-B Cells

(A) Diagram of the C57Bl/6 *Igh* locus is shown with genomic distances (Johnston et al., 2006). The BAC probes used in FISH studies are indicated by the blue, red, and green lines below the *Igh* locus. Topological subdomains A (114,665,117–115,239,000), B (115,239,000–115,949,000), and C (116,069,000–116,874,000), and all genomic coordinates are chr12, mm9. The *Igh* locus contains approximately 100 V_H gene segments that span 2.4 Mb. The interspersed distal V_H segments at the 5′ end of the locus are composed of the J558 and 3609 families. The 7183 family is located at the proximal end of the locus. The intermediate V_H segments are composed of the S107 family along with nine smaller V_H families. Representative V_H gene segments are positioned above the locus, Vh81.X (Vh7183.2.3; 114816717–114817010), 5′7183 (Vh7183.20.37; 115097360–115097653), 3′558 (VhJ558.1.85; 115707286–115707582), J558.88.194 (VhJ558.88.194; 117238239–117238532). The vertical blue bar on the locus located between the constant region genes (C_H) and 7183 V_H segments contains the joining (J_H) and diversity (D_H) gene segments. The C_H genes encode *Igh* isotypes and span an additional 220 kb. Not shown: Eμ is located between the J_H and C_H gene segments and 3′Eα an enhancer at the 3′ end of the locus.

(B) Three-color FISH using purified bone-marrow Rag2-deficient pro-B cells. BAC probes are indicated in (A) and color coded as indicated. A representative nucleus is shown. Probes labeled with Alexa Fluor 594 (red), 488 (green), and Alexa Fluor 697 (blue) were hybridized to fixed pro-B cells. Probe signals were from epifluorescence microscopy, and the distances between probes were computed as described (Jhunjhunwala et al., 2008). Probes combinations were red and green (RI-RII) and red and blue (H14-RI).

(C) Quantitation of FISH data. The distance between the red, green, and blue FISH signals shown in (B) for 100–300 alleles were divided into four categories: <0.3, 0.31–0.5, 0.51–0.8, and 0.81–1.0 μm. The percentage of *Igh* alleles in each category was determined (y axis) for each probe combination and is represented in different colors. Probe combinations are indicated on the x axis below the histograms. Purified pro-B cells from at least three mice were used for each experiment.

(D) (Left panel) Cumulative frequency analyses are for each probe combination. (Right panel) Boxplots indicate the first and third quartiles, and the band inside the box is the median distance between the probes. The whiskers indicate the ninth and 91st percentiles for probe distances, and outliers are indicated by the dots. p values were calculated using the Mann-Whitney U test. ***$p < 0.0001$.

(E) Three-color FISH using purified BM pro-B and non-B cells on the Rag2-deficient background. Cells are from at least three mice. BAC probes are shown in (A). Probes combinations were red and green (RI-RII), red and blue (RI-RIII), and green and blue (RII-RIII).

(F) Quantitation of FISH data. 3D FISH signals shown in (E) for ~100–300 alleles were quantitated as described in (C). Probe combinations are shown above the histograms.

(G and H) p values are calculated in Kolmogorov-Smirnov and the Wilcoxon tests (see Table S6). Cumulative frequency analyses (G) and boxplots (H) are shown for each probe combination in each cell type. P = pro-B, N = non-B in (H).

additional 12% alleles, as compared to 29% in pro-B cells (Figure 4C, insets a and a.1). Moreover, in non-B lineage cells the most prevalent configuration of alleles positioned probes RI-RII-RIII at a distance (42% compared to 1% in pro-B cells) (Figure 4C, inset e), presumably reflecting linear un-contracted loci in these cells. Notably, probes RII-RIII are pairwise associated in 20% of alleles of non-B lineage cells, whereas this configuration occurs in only 3.5% of pro-B cell alleles (Figure 4B, inset d, and Figure 4C, inset d). The presence of frequent RII-RIII interactions in non-B lineage cells implies that the J558 V_H gene family is compacted in accord with the 5C findings (Figure 2). We conclude that spatial aggregation of sites I-II-III is

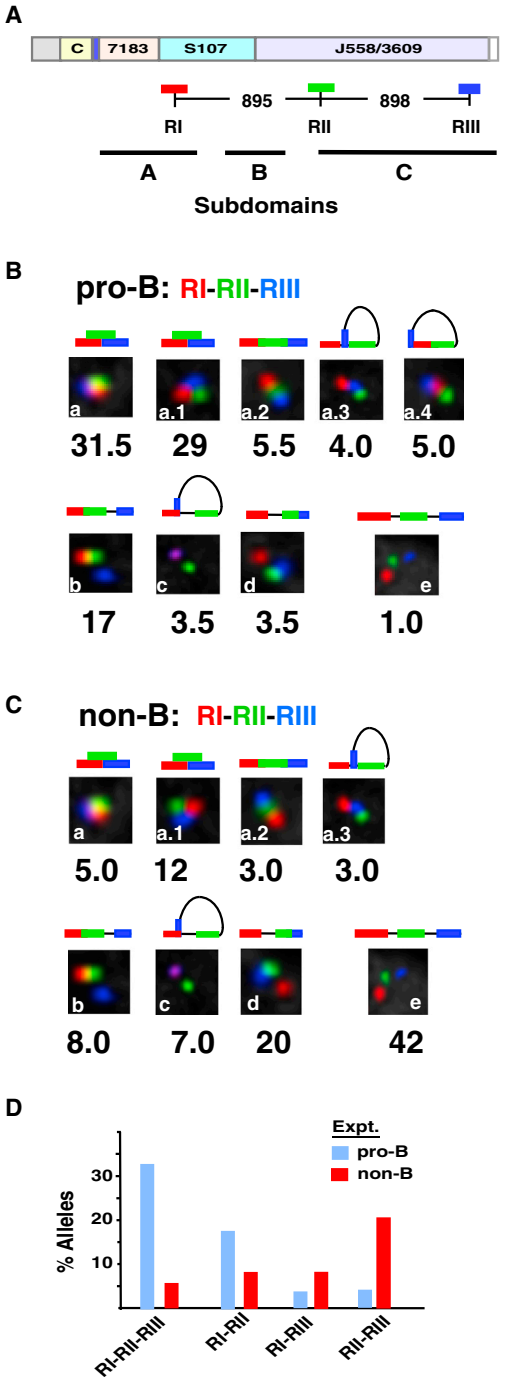

Figure 4. Sites I-II-III Are Selectively Superimposed in Pro-B Cells

Three-color FISH data for ~200 nuclei for each probe set. Allele configurations and probe distances are defined in Figure S6. Purified pro-B cells from at least three mice were used for each of two experiments. p values are derived in Kolmogorov-Smirnov and the Wilcoxon tests (see Table S6).

(A) A schematic of the WT *Igh* locus with genomic distances between BAC probes. The probes combinations are RI (red), RII (green), and RIII (blue). The topological subdomains A, B, and C that are derived from the 5C studies shown in Figure 2 are arrayed at bottom.

(B and C) BAC probes RI, RII, and RIII, labeled as indicated, were hybridized simultaneously to Rag2-deficient pro-B cells (B) or non-B cells (C) from bone marrow of Rag2-deficient mice. The percentage of *Igh* alleles in various spatial configurations as schematized above each inset is indicated.

(D) Histograms summarizing the three-color FISH results shown in (B) and (C) using the probe combinations RI, RII, and RIII for pro-B cells (blue bars) and non-B lineage cells (red bars) (x axis). The percentage of alleles in which two- or three-probes are superimposed or in very close contact are indicated (y axis).

pro-B-selective and that these interactions may comprise important determinants of V_H locus compaction (Figure 4D).

Meta-Loop Formation through Sites I, II, and III Is Eμ Independent

The tissue-specific Eμ enhancer is required for V(D)J joining (Afshar et al., 2006; Perlot et al., 2005) and for mediating a subset of long-range chromatin interactions that contribute to locus compaction (Guo et al., 2011a). Earlier studies showed that Eμ interacted with two sites in the V_H region (Guo et al., 2011a). One of these sites, 5′7183, lies close to RI identified in this study; the other, referred to as 3′558, lies between RI and RII (Figures 3A and 5A). We had proposed that Eμ-5′7183 and Eμ-3′558 associations bring the V_H region close to the DJ_H part of the locus to facilitate V_H recombination (Guo et al., 2011a). Our current observations suggested two possibilities: (1) that RI-II-III interactions were a part of Eμ-dependent locus contraction or (2) that RI-II-III interactions folded the V_H domain independent of Eμ. To distinguish between these possibilities, we performed three-color 3D FISH to measure RI-II-III associations on *Igh* alleles with defined deletions.

We used P^-E^+ alleles that lack a promoter associated with the 3′ most D_H gene segment DQ52 and P^-E^- alleles that lack both the DQ52 promoter and Eμ (Afshar et al., 2006). P^-E^+ alleles behave indistinguishably from WT *Igh* alleles in most epigenetic and locus conformation assays, whereas P^-E^- alleles are substantially different (Guo et al., 2011a). We therefore attribute differences between these two alleles to the presence, or absence, of Eμ. Both *Igh* genotypes were examined in a RAG2-deficient context to preserve the locus in an unchanged configuration. Using purified primary pro-B cells, we found that FISH signals from RI (red), RII (green), and RIII (blue) probes were virtually superimposable for both P^-E+ or P^-E^- *Igh* alleles (Figure 5B and quantified in Figures 5C and 5D; also see Table S6). We conclude that interactions between sites I-III represent Eμ-independent looping within the V_H locus.

Site-I-III-Mediated Looping Is Pax5 Dependent

Contraction of the *Igh* locus in pro-B cells is altered by the transcription factor, Pax5 (Fuxa et al., 2004). This effect is thought to be mediated by Pax5 binding to a series of 14 Pax5-associated intergenic repeat (PAIR) sequences that are spread across 750 kb spanning the distal J558 V_H genes. PAIR motifs are composed of Pax5, E2A, and CTCF binding sites (Ebert et al., 2011). Sites II.5 and III overlap with PAIR 6–8 and 10–11, respectively. PAX5 occupancy has been detected at these sites in vivo (Ebert et al., 2011). However, the means by which Pax5 binding to PAIR elements contracts the locus remains unclear. Because specific chromatin interaction sites that mediate *Igh* locus contraction have not been identified, one working model is that

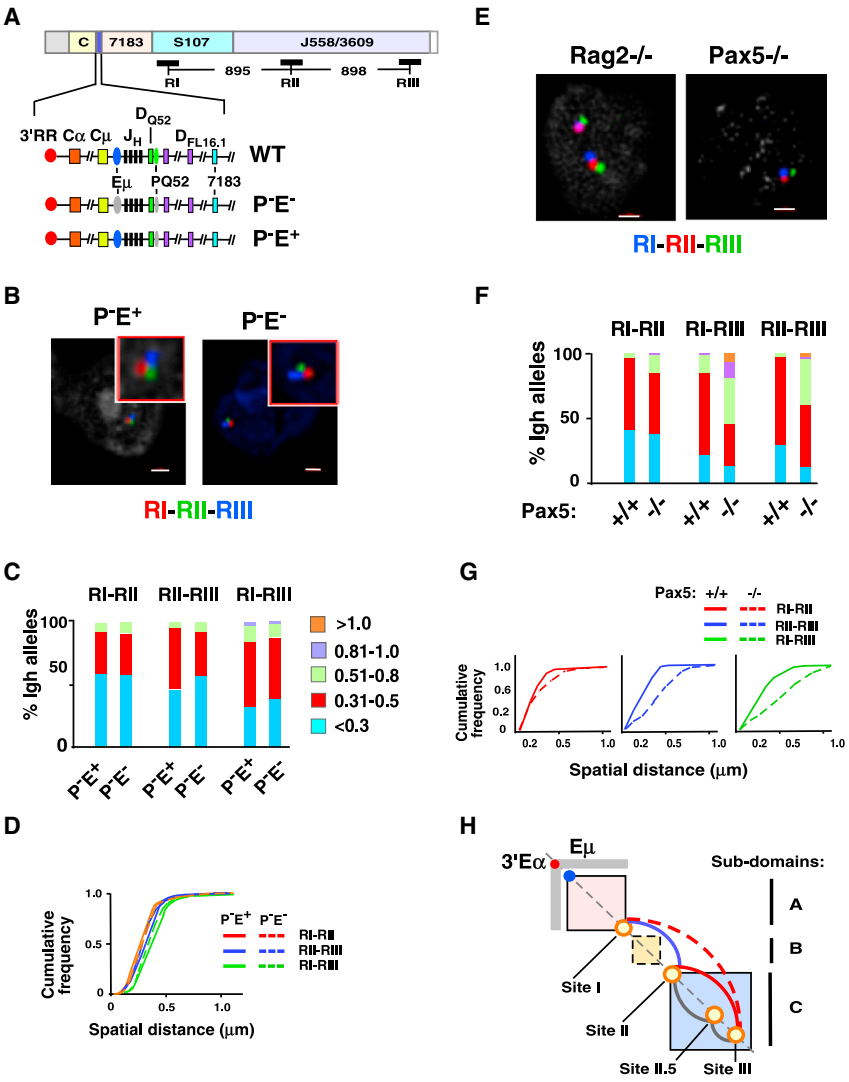

Figure 5. Locus Contraction Mediated by Sites I-II-III Is Eμ Independent but Requires Pax5

(A) A diagram of the *Igh* locus indicates the location and distances between the three FISH probes RI, RII, and RIII. The lower three lines show an expanded section of the *Igh* locus from 3′RR through the D_H cluster and ending with the proximal V_H gene segment, 7183. Eμ (blue oval) is a transcription enhancer located in the J_H-Cμ intron, and PQ52 (green oval) is a promoter associated with the 3′ most D_H gene segment, DQ52. Deletions of PQ52 (P^-) and/or Eμ (E^-) are indicated (gray ovals).

(B) Three-color FISH using purified Rag-deficient pro-B cells that are deleted for PQ52 (P^-E^+) and for both PQ52 and Eμ (P^-E^-). BAC probes are RI (red), RII (green), and RIII (blue). A representative nucleus is shown for each genotype. Probe contacts were red and green (RI-RII), red and blue (RI-RIII), and green and blue (RII-RIII).

(C) Quantitation of FISH data. The distance between the red, green, and blue FISH signals shown in (B) for ~200 nuclei were divided into five categories: <0.3, 0.31–0.5, 0.51–0.8, 0.81–1.0, and >1.0 μm. The percentage of *Igh* alleles in each category (y axis) for each *Igh* genotype (x axis) is represented in different colors. Probe combinations are shown above the histograms. Purified pro-B cells from at least three mice were used for each experiment. Data are from at least two independent experiments.

(D) Cumulative frequency analyses are shown for each probe combination, and the genotypes are indicated. p values are defined by Kolmogorov-Smirnov and Wilcoxon tests (see Table S6).

(E) Three-color FISH using $Rag2^{-/-}$ or $Pax5^{-/-}$ pro-B cells and BAC probes are as in (A) and were labeled as follows: RI (blue), RII (red), and RIII (green). Representative nuclei from each genotype are shown.

(F) Distances between the probe signals were analyzed in ~100 nuclei.

(G) Cumulative frequency analyses are shown. p values are summarized in Table S6.

(H) A diagram of *Igh* topological subdomains A (pink box), B (yellow box), and C (blue box). Eμ (blue dot), 3′Eα (red dot), and sites I, II, II.5, and III (orange circles) are located along the diagonal. The gray rectangular arms extending from 3′Eα indicate increased 5C interactions in pro-B cells. Loops that anchored at sites I, II, II.5, and III and that are Pax5 dependent (red, dashed red), Pax5 independent (blue), and not tested (gray).

locus contraction occurs by mechanisms that are distinct from classical chromatin looping (Medvedovic et al., 2013). Therefore, it was of significant interest to determine the role of Pax5 in chromatin looping at sites I, II, and III. For this, we carried out FISH with probes RI (blue), RII (red), and RIII (green) in pro-B cells from RAG2-deficient and Pax5-deficient mice (Figures 5A and 5E). We found that Pax5 deficiency had little impact on RI-RII pairwise association but significantly disrupted interactions between sites II-III as well as sites I-III (Figures 5F and 5G; also see Table S6). We conclude that Pax5 ensures interactions between sites II and III (Figure 5H, red line). When this interaction is disrupted in the absence of Pax5, the anchor sites I-II are released from site III, thereby altering the spatial distance between sites I and III. That is, Pax5-independent interactions between site I-II and Pax5-dependent interactions between site II-III bring all three sites together in pro-B cells. Alternatively, site I may also directly interact with site III in a Pax5-dependent manner (Figure 5H, dashed red line). Our three-color FISH studies indicate that interactions between sites I-III and II-III are infrequent, whereas the three-way association of sites I-II-III is the most prevalent looping configuration in pro-B cell nuclei (Figure 4D). Looping between sites I and II is the next most frequent interaction and also very prevalent (Figure 4D). Thus, we favor a model in which Pax5 facilitates locus contraction by promoting looping of site III with sites I and II (Figure 5H).

DISCUSSION

Our studies define several levels of topological fine structure within the *IgH* TAD/LAD that provide unique insights into the 3D architecture of the locus. First, HiC studies indicate that the *Igh* locus is encompassed within an i-TOF at the pro-B cell stage

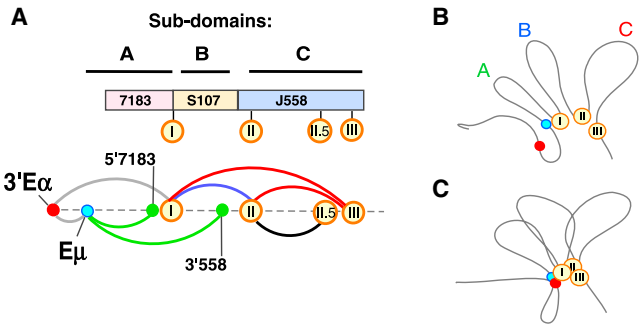

Figure 6. Site I Coordinates V_H Locus Contraction

(A) (Top) Topological subdomains A–C and V_H gene families are drawn approximately to scale. Sites I, II, II.5, and III (orange circles) are aligned with their positions in topological subdomains and with respect to V_H gene families. (Bottom) Meta-looping interactions anchored at sites I, II, II.5, and III (orange circles) are Pax5 dependent (red arc), independent (blue arc), and not tested (black arc). Green arcs, Eμ-dependent loops (Guo et al., 2011a); gray arc, 3′Eα loops with Eμ (Kumar et al., 2013) and site I.

(B and C) Diagrams of subdomain A, B, and C. Sites I, II, and III (orange circles). Dots indicate 3′Eα (red) and Eμ (teal). (B) Non-B cells: topological subdomains A, B, and C are in an extended configuration. (C) In pro-B cells, site I loops with sites II and III and with Eμ and 3′Eα to contract the locus.

of development. Second, 5C studies reveal three distinct topological subdomains in pro-B cells and MEFs (Figure 6). Subdomain A, which covers approximately 440 kb, extends from Eμ to the newly identified site I. Subdomain C covers ~1.1 Mb and extends between newly identified sites II and III. Extensive intra-domain contacts are evident within these two domains. The region between sites I and II, that we refer to as subdomain B, differs from the other two domains in having many fewer intra-domain contacts.

Subdomain A, which encompasses proximal V_H genes, in MEFs becomes subsumed within a larger subdomain that extends from site I to near the 3′Eα enhancer at the 3′ end of the *Igh* locus in pro-B cells. These differences reflect chromatin interactions with the B lineage-specific Eμ and 3′Eα enhancers in pro-B cells. Eμ and 3′Eα were previously shown to interact together as well as with the 5′ end of the VH7183 gene family (Guo et al., 2011a; Kumar et al., 2013). Several earlier observations have shown that proximal V_H genes are regulated differently from the rest of the V_H genes. Proximal V_H genes recombine normally, whereas distal V_H gene recombination is reduced in Pax5-, YY1-, and Ezh2-deficient pro-B cells (Fuxa et al., 2004; Hesslein et al., 2003; Liu et al., 2007; Reynaud et al., 2008). Thus, encapsulation of proximal V_H genes together with the D_H/J_H part of the locus within subdomain A may, in part, distinguish them from distal V_H genes that lie within subdomain C.

Intra-domain contacts within subdomain C occur in pro-B cells and MEFs. Earlier evidence suggests that CTCF, cohesin, and Mediator-1 anchor constitutive architectural chromatin contacts between and within constitutive topological subdomains (Phillips-Cremins et al., 2013). However, the *Igh* locus, including the expanse of subdomain C, is devoid of these factors prior to the pro-B cell stage of development. We infer that constitutive topologies may be mediated by other, as-yet-undefined, means.

Third, our 5C and FISH studies identify long-range, B lineage-specific interactions between subdomains (Figure 6A, blue and red arcs). These interactions, that we term meta-loops, serve to bring the three subdomains into spatial proximity in pro-B cells (Figures 6B and 6C). The importance of interactions between sites I, II, and III is revealed in the juxtaposition of all three sites in approximately 60% of pro-B cells compared to <20% non-B cells. As a consequence, the entire V_H region is brought into proximity of the D_H/J_H region of the locus to enable comparable access of all V_H gene segments for recombination. It is intriguing that a small proportion of sites I, II, and III are also in close proximity in non-B cells. One possibility is that this is stochastic. An interesting alternate possibility is that these regions are favored sites of interaction in non-B cells as well, and it is only the frequency of interaction that changes in pro-B cells. In other words, pro-B cells utilize constitutively favored interactions to maximize locus compaction. The binding of architectural proteins, such as CTCF and Pax5, at sites I, II, and III in pro-B cells may facilitate such interactions.

Fourth, we demonstrate that Pax5 is essential to bring site III into contact with sites I and II (Figure 6A, red arcs). Since site I-II interactions are unaffected in Pax5-deficient pro-B cells, we conclude that Pax5 primarily drives interactions with site III. It is noteworthy that the 14 PAIR elements that were proposed to mediate locus compaction via Pax5 are all located in the genomic region spanning subdomain C and PAIR motifs 10 and 11 overlap with site III (Ebert et al., 2011). In the absence of site III interactions, VHJ558 gene segments (subdomain C) fail to gain proximity to site I and subdomain A providing a plausible explanation for reduced VHJ558 rearrangements in Pax5-deficient pro-B cells. We also note that V_H locus compaction, revealed as three-way interaction between sites I, II, and III does not require the intronic enhancer Eμ.

Since the pioneering studies of Kosak et al., it is clear that the 5′ and 3′ ends of the *Igh* locus are closer in pro-B cells compared to other non-B lineage cells (Kosak et al., 2002). The term locus compaction/contraction is frequently used to refer to this phenomenon. A recent HiC study was interpreted to suggest that in pro-B cells the 3′ end regulatory region (3′ RR) located at the Igh locus boundary may function as a super-anchor that creates proximity between proximal and distal gene segments based on numerous CTCF-directed looping interactions along the length of the locus (Benner et al., 2015). However, HiC analyses are relatively low resolution due to sequencing depth limitations in conjunction with very large binning windows (≥100 kb) and therefore lack the sensitivity to identify interactions between specific motifs or determine whether those contacts are direct or indirect. An important conceptual point that emerges from our high-resolution 5C studies is that locus compaction is the result of several overlapping phenomena that are mediated by discrete and independent chromatin loops. We propose that meta-loops serve to compact the conserved topological folds of subdomains A–C. The topological folds may gain their structure in pro-B cells via CTCF-dependent short-range locus compaction. Thus, partial locus compaction and its consequences are evident in special circumstances. Pax5-induced locus compaction (Fuxa et al., 2004) is focused on site III and only affects distal V_H genes, whereas Eμ-dependent locus

compaction (Guo et al., 2011a) affects interaction between the 3′ *Igh* region (subdomain A) and the V_H region (Figure 6A, green arcs). Accordingly, only distal V_H gene recombination is affected in Pax5-deficient cells (Hesslein et al., 2003). Because Eμ deletion is pleiotropic, its effect on V_H recombination per se is difficult to deconvolute. In summary, we propose that the *Igh* locus is contracted by means of meta-loops that are anchored at sites I-III and are mediated by distinct genetic factors.

EXPERIMENTAL PROCEDURES

Mice and Primary Cell Culture and Cell Lines and FISH

P^-E+ and P^-E^- mice were previously described (Afshar et al., 2006). Rag-deficient mice on the C57BL/6 background were from Jackson Laboratory or maintained in colonies at the University of Illinois College of Medicine, or the NIA, NIH. All mouse procedures were approved by the Institutional Animal Care Committee of the University of Illinois College of Medicine, or the NIA, NIH animal facilities, in accordance with protocols approved by the UIC or NIA Institutional Animal Care and Use Committees. For all other pro-B cell analyses, $Rag2^{-/-}$ pro-B cells were cultured as previously described (Sayegh et al., 2005) with minor modifications. $CD19^+$ cells were isolated using anti-CD19-coupled magnetic beads (Miltenyi) and cultured in the presence of interleukin 7 (IL-7) (1% v/v supernatant of a J558L cell line stably expressing IL-7) for 4 days. Pax5-deficient pro-B cells were kindly provided by Dr. J. Pongubala. The Abelson-MuLV-transformed pro-B cell line was D345 (Ji et al., 2010). FISH was performed as described (Guo et al., 2011a). Additional experimental details are available online in Supplemental Experimental Procedures.

Hi-C and 5C Libraries and Analyses

HiC libraries derived from A-MuLV-transformed cell lines that were previously described (Bredemeyer et al., 2006; Zhang et al., 2012). 5C library construction was performed as described (Dostie and Dekker, 2007; Kumar et al., 2013) (Supplemental Experimental Procedures).

ACCESSION NUMBERS

The accession number for the 5C sequence data reported in this paper is GEO: GSE76086.

SUPPLEMENTAL INFORMATION

Supplemental Information includes Supplemental Experimental Procedures, six figures, and six tables and can be found with this article online at http://dx.doi.org/10.1016/j.celrep.2015.12.083.

AUTHOR CONTRIBUTIONS

Conceptualization, A.L.K. and R.S.; Methodology, A.L.K., R.W., R.S., and J.D.; Investigation, R.W., L.M., and T.G.; Writing–Original Draft, A.L.K.; Writing–Review & Editing A.L.K. and R.S.; Funding Acquisition, A.L.K. and R.S., Formal Analysis, D.R., J.L., J.D., and B.L.; Resources, C.G., S.D., W.W., and K.G.B.; Supervision, A.L.K. and R.S.

ACKNOWLEDGMENTS

This work was supported by the National Institutes of Health (RO1AI052400, R21AI117687 to A.K., HG003143 and HG00459 to J.D., GM079804 to J.L.), National Science Foundation (DBI 1062328 and MCB-1415589 to J.L.), the Chicago Biomedical Consortium with support from the Searle Funds at The Chicago Community Trust (to A.K. and J.L.), the W.M. Keck Foundation (to J.D.), and Intramural Research Program of the National Institute on Aging (Baltimore, MD) (to R.S.). We thank G. Gursoy for helpful discussions and Dr. J. Pongubala for the Pax5-deficient pro-B cell line.

Received: August 31, 2015
Revised: October 29, 2015
Accepted: December 16, 2015
Published: January 21, 2016

REFERENCES

Afshar, R., Pierce, S., Bolland, D.J., Corcoran, A., and Oltz, E.M. (2006). Regulation of IgH gene assembly: role of the intronic enhancer and 5′DQ52 region in targeting DHJH recombination. J. Immunol. *176*, 2439–2447.

Belmont, A.S. (2014). Large-scale chromatin organization: the good, the surprising, and the still perplexing. Curr. Opin. Cell Biol. *26*, 69–78.

Benner, C., Isoda, T., and Murre, C. (2015). New roles for DNA cytosine modification, eRNA, anchors, and superanchors in developing B cell progenitors. Proc. Natl. Acad. Sci. USA *112*, 12776–12781.

Bickmore, W.A., and van Steensel, B. (2013). Genome architecture: domain organization of interphase chromosomes. Cell *152*, 1270–1284.

Bredemeyer, A.L., Sharma, G.G., Huang, C.Y., Helmink, B.A., Walker, L.M., Khor, K.C., Nuskey, B., Sullivan, K.E., Pandita, T.K., Bassing, C.H., and Sleckman, B.P. (2006). ATM stabilizes DNA double-strand-break complexes during V(D)J recombination. Nature *442*, 466–470.

Cuddapah, S., Jothi, R., Schones, D.E., Roh, T.Y., Cui, K., and Zhao, K. (2009). Global analysis of the insulator binding protein CTCF in chromatin barrier regions reveals demarcation of active and repressive domains. Genome Res. *19*, 24–32.

Degner, S.C., Wong, T.P., Jankevicius, G., and Feeney, A.J. (2009). Cutting edge: developmental stage-specific recruitment of cohesin to CTCF sites throughout immunoglobulin loci during B lymphocyte development. J. Immunol. *182*, 44–48.

Degner, S.C., Verma-Gaur, J., Wong, T.P., Bossen, C., Iverson, G.M., Torkamani, A., Vettermann, C., Lin, Y.C., Ju, Z., Schulz, D., et al. (2011). CCCTC-binding factor (CTCF) and cohesin influence the genomic architecture of the Igh locus and antisense transcription in pro-B cells. Proc. Natl. Acad. Sci. USA *108*, 9566–9571.

Dixon, J.R., Selvaraj, S., Yue, F., Kim, A., Li, Y., Shen, Y., Hu, M., Liu, J.S., and Ren, B. (2012). Topological domains in mammalian genomes identified by analysis of chromatin interactions. Nature *485*, 376–380.

Dostie, J., and Dekker, J. (2007). Mapping networks of physical interactions between genomic elements using 5C technology. Nat. Protoc. *2*, 988–1002.

Ebert, A., McManus, S., Tagoh, H., Medvedovic, J., Salvagiotto, G., Novatchkova, M., Tamir, I., Sommer, A., Jaritz, M., and Busslinger, M. (2011). The distal V(H) gene cluster of the Igh locus contains distinct regulatory elements with Pax5 transcription factor-dependent activity in pro-B cells. Immunity *34*, 175–187.

Fuxa, M., Skok, J., Souabni, A., Salvagiotto, G., Roldan, E., and Busslinger, M. (2004). Pax5 induces V-to-DJ rearrangements and locus contraction of the immunoglobulin heavy-chain gene. Genes Dev. *18*, 411–422.

Gibcus, J.H., and Dekker, J. (2013). The hierarchy of the 3D genome. Mol. Cell *49*, 773–782.

Guo, C., Gerasimova, T., Hao, H., Ivanova, I., Chakraborty, T., Selimyan, R., Oltz, E.M., and Sen, R. (2011a). Two forms of loops generate the chromatin conformation of the immunoglobulin heavy-chain gene locus. Cell *147*, 332–343.

Guo, C., Yoon, H.S., Franklin, A., Jain, S., Ebert, A., Cheng, H.L., Hansen, E., Despo, O., Bossen, C., Vettermann, C., et al. (2011b). CTCF-binding elements mediate control of V(D)J recombination. Nature *477*, 424–430.

Hesslein, D.G., Pflugh, D.L., Chowdhury, D., Bothwell, A.L., Sen, R., and Schatz, D.G. (2003). Pax5 is required for recombination of transcribed, acetylated, 5′ IgH V gene segments. Genes Dev. *17*, 37–42.

Jhunjhunwala, S., van Zelm, M.C., Peak, M.M., Cutchin, S., Riblet, R., van Dongen, J.J., Grosveld, F.G., Knoch, T.A., and Murre, C. (2008). The 3D structure of the immunoglobulin heavy-chain locus: implications for long-range genomic interactions. Cell *133*, 265–279.

Ji, Y., Resch, W., Corbett, E., Yamane, A., Casellas, R., and Schatz, D.G. (2010). The in vivo pattern of binding of RAG1 and RAG2 to antigen receptor loci. Cell *141*, 419–431.

Johnston, C.M., Wood, A.L., Bolland, D.J., and Corcoran, A.E. (2006). Complete sequence assembly and characterization of the C57BL/6 mouse Ig heavy chain V region. J. Immunol. *176*, 4221–4234.

Kosak, S.T., Skok, J.A., Medina, K.L., Riblet, R., Le Beau, M.M., Fisher, A.G., and Singh, H. (2002). Subnuclear compartmentalization of immunoglobulin loci during lymphocyte development. Science *296*, 158–162.

Kumar, S., Wuerffel, R., Achour, I., Lajoie, B., Sen, R., Dekker, J., Feeney, A.J., and Kenter, A.L. (2013). Flexible ordering of antibody class switch and V(D)J joining during B-cell ontogeny. Genes Dev. *27*, 2439–2444.

Lieberman-Aiden, E., van Berkum, N.L., Williams, L., Imakaev, M., Ragoczy, T., Telling, A., Amit, I., Lajoie, B.R., Sabo, P.J., Dorschner, M.O., et al. (2009). Comprehensive mapping of long-range interactions reveals folding principles of the human genome. Science *326*, 289–293.

Lin, Y.C., Benner, C., Mansson, R., Heinz, S., Miyazaki, K., Miyazaki, M., Chandra, V., Bossen, C., Glass, C.K., and Murre, C. (2012). Global changes in the nuclear positioning of genes and intra- and interdomain genomic interactions that orchestrate B cell fate. Nat. Immunol. *13*, 1196–1204.

Liu, H., Schmidt-Supprian, M., Shi, Y., Hobeika, E., Barteneva, N., Jumaa, H., Pelanda, R., Reth, M., Skok, J., Rajewsky, K., and Shi, Y. (2007). Yin Yang 1 is a critical regulator of B-cell development. Genes Dev. *21*, 1179–1189.

Medvedovic, J., Ebert, A., Tagoh, H., Tamir, I.M., Schwickert, T.A., Novatchkova, M., Sun, Q., Huis In 't Veld, P.J., Guo, C., Yoon, H.S., et al. (2013). Flexible long-range loops in the VH gene region of the Igh locus facilitate the generation of a diverse antibody repertoire. Immunity *39*, 229–244.

Nora, E.P., Lajoie, B.R., Schulz, E.G., Giorgetti, L., Okamoto, I., Servant, N., Piolot, T., van Berkum, N.L., Meisig, J., Sedat, J., et al. (2012). Spatial partitioning of the regulatory landscape of the X-inactivation centre. Nature *485*, 381–385.

Peric-Hupkes, D., Meuleman, W., Pagie, L., Bruggeman, S.W., Solovei, I., Brugman, W., Gräf, S., Flicek, P., Kerkhoven, R.M., van Lohuizen, M., et al. (2010). Molecular maps of the reorganization of genome-nuclear lamina interactions during differentiation. Mol. Cell *38*, 603–613.

Perlot, T., Alt, F.W., Bassing, C.H., Suh, H., and Pinaud, E. (2005). Elucidation of IgH intronic enhancer functions via germ-line deletion. Proc. Natl. Acad. Sci. USA *102*, 14362–14367.

Phillips-Cremins, J.E., Sauria, M.E., Sanyal, A., Gerasimova, T.I., Lajoie, B.R., Bell, J.S., Ong, C.T., Hookway, T.A., Guo, C., Sun, Y., et al. (2013). Architectural protein subclasses shape 3D organization of genomes during lineage commitment. Cell *153*, 1281–1295.

Reynaud, D., Demarco, I.A., Reddy, K.L., Schjerven, H., Bertolino, E., Chen, Z., Smale, S.T., Winandy, S., and Singh, H. (2008). Regulation of B cell fate commitment and immunoglobulin heavy-chain gene rearrangements by Ikaros. Nat. Immunol. *9*, 927–936.

Sayegh, C.E., Jhunjhunwala, S., Riblet, R., and Murre, C. (2005). Visualization of looping involving the immunoglobulin heavy-chain locus in developing B cells. Genes Dev. *19*, 322–327.

Seitan, V.C., and Merkenschlager, M. (2011). Cohesin and chromatin organisation. Curr. Opin. Genet. Dev.

Zhang, Y., McCord, R.P., Ho, Y.J., Lajoie, B.R., Hildebrand, D.G., Simon, A.C., Becker, M.S., Alt, F.W., and Dekker, J. (2012). Spatial organization of the mouse genome and its role in recurrent chromosomal translocations. Cell *148*, 908–921.

Zullo, J.M., Demarco, I.A., Piqué-Regi, R., Gaffney, D.J., Epstein, C.B., Spooner, C.J., Luperchio, T.R., Bernstein, B.E., Pritchard, J.K., Reddy, K.L., and Singh, H. (2012). DNA sequence-dependent compartmentalization and silencing of chromatin at the nuclear lamina. Cell *149*, 1474–1487.